Comparison of FRF and Modal Methods for Combining Experimental and Analytical Substructures

Matthew S. Allen[1] and Randall L. Mayes[2]
[1]University of Wisconsin-Madison, Corresponding Author: msallen@cae.wisc.edu
[2] Sandia National Laboratories*, rlmayes@sandia.gov

Abstract:

This paper investigates methods for coupling analytical dynamic models of subcomponents with experimentally derived models in order to predict the response of the combined system, focusing on modal substructuring or Component Mode Synthesis (CMS), the experimental analog to the ubiquitous Craig-Bampton method. While the basic methods for combining experimental and analytical models have been around for many years, it appears that these are not often applied successfully. The CMS theory is presented along with a new strategy, dubbed the Maximum Rank Coordinate Choice (MRCC), that ensures that the constrained degrees of freedom can be found from the unconstrained without encountering numerical ill conditioning. The experimental modal substructuring approach is also compared with frequency response function coupling, sometimes called admittance or impedance coupling. These methods are used both to analytically remove models of a test fixture (required to include rotational degrees of freedom) and to predict the response of the coupled beams. Both rigid and elastic models for the fixture are considered. Similar results are obtained using either method although the modal substructuring method yields a more compact database and allows one to more easily interrogate the resulting system model to assure that physically meaningful results have been obtained. A method for coupling the fixture model to experimental measurements, dubbed the Modal Constraint for Fixture and Subsystem (MCFS) is presented that greatly improves the result and robustness when an elastic fixture model is used.

1. Introduction

Modal substructuring or Component Mode Synthesis (CMS) has been standard practice for many decades in the analytical realm. Countless works have treated the subject with regards to Finite Element model reduction, where component models are used to create reduced order models of complex subsystems. A wide variety of flavors of Component Mode Synthesis are available, the most common apparently being that by Craig and Bampton [1, 2]. Many standard texts on vibratory systems or modal analysis treat this subject [1, 3, 4]. Using these methods, accurate models of complex systems have been created with orders of magnitude fewer degrees of freedom than would have been required if model reduction had not been employed. A number of works have also investigated the possibility of applying the methods to nonlinear systems with promising results [5, 6].

There has also been considerable interest in creating models from experimental measurements that can be combined with analytical models. Subcomponents are often designed by a number of independent groups that do not have the information or the resources to model the macro system. In other applications some particular components may be too difficult to model analytically with the required precision. A number of researchers have investigated the possibility of combining analytical and experimental models. Martinez, Miller and Carne used

* Sandia is a multiprogram laboratory operated by Sandia Corporation, a Lockheed Martin Company, for the United States Department of Energy's National Nuclear Security Administration under Contract DE-AC04-94AL85000.

these methods to couple experimental models for a beam like system and a shell-payload system [7]. Urgueira compared the modal substructuring approach with the impedance (or admittance) coupling approach treating issues such as the need for residual compliances when free modes are used and the difficulty in measuring rotations [8]. The more recent doctoral work by Ind [9] is most relevant to this work; he investigated the possibility of determining the response of a delicate subcomponent by attaching a fixture, testing the combined system and then using a variety of methods to remove the effects of the test fixture from the measured responses. All of these works showed promising results, while also indicating significant difficulties in obtaining the required responses with sufficient precision, such as rotational and residual responses, in dealing with uncertainties, and in avoiding numerical ill conditioning and non-physicality in the responses. Very large errors were sometimes obtained due to small errors in the subcomponent models [10].

This paper presents a subset of work performed at Sandia National Laboratories, aimed at revisiting these issues on a simple system in an effort to better establish the procedures and methodologies so that these methods can be used with more confidence. A system similar to that discussed here was previously investigated by Simmons, Smith, Mayes and Epp in [11], demonstrating how sensitive the admittance or impedance coupling method can be to experimental errors when dealing with lightly damped structures. This paper compares the modal substructuring or Component Mode Synthesis (CMS) approach with the FRF coupling admittance (or impedance) approach. The CMS method is employed using both free-free and mass-loaded-interface modes in an analytical study and using only the latter in the experimental study. A companion paper discusses the experimental issues addressed and presents more detailed admittance coupling results [12].

This paper is organized as follows. The modal substructuring theory is briefly presented in Section 2, along with the Maximum Rank Coordinate Choice (MRCC) method that avoids ill conditioning when enforcing constraints between structures. A method is also presented that joins the modal degrees of freedom of a fixture to the measured responses on a subcomponent that has been dubbed the Modal Constraint for Fixture and Subsystem (MCFS). The system of interest is discussed in Section 3, followed by an analytical study using finite element models in Section 4. The experimental results are also presented, and finally some conclusions in Section 5.

2. Theory

2.1. Component Mode Synthesis

The basic modal substructuring or Component Mode Synthesis theory will be presented briefly for convenience, following the notation used in Ginsberg [3]. Modal substructuring is best understood in the context of the Ritz series. The modal models for each subcomponent define $N \times N$ mass, stiffness and (sometimes) damping matrices for the subcomponent, where N is the number of modes in the model of the substructure. As in the Ritz method, the number of physical degrees of freedom or node points N_p associated with the modal model may not be the same as the number of modes N. The model for each subcomponent is uniquely defined by its modal parameters where each mode is defined by its natural frequency ω_r and mode vector $\{\phi_r\}$. The damping matrix can be defined by augmenting this set with the modal damping ratios ζ_r or loss factors for viscous modal damping or structural damping models respectively. A non-proportional damping model requires the modal damping ratios and a set of complex mode vectors in place of the real mode vectors $\{\phi_r\}$ to complete the state space description [3]. The discussion here will be confined to real mode vectors and modal damping for simplicity, although the extension to state space is relatively straightforward.

The modal parameters define a model for each subsystem, whose equations of motion are the following if the mode vectors $\{\phi_r\}$ are mass normalized

$$\begin{aligned}
[I]\{\ddot{q}\}+\left[\backslash 2\zeta_r\omega_{r\backslash}\right]\{\dot{q}\}+\left[\backslash \omega_r^{\,2}{}_{\backslash}\right]\{q\} &= [\Phi]^T\{F\} \\
\{y\} &= [\Phi]\{q\} \\
[\Phi] &= \left[\{\phi_1\} \quad \cdots \quad \{\phi_N\}\right]
\end{aligned} \tag{1},$$

where *[I]* is an NxN identity matrix and $\left[\backslash 2\zeta_r\omega_{r\backslash}\right]$ and $\left[\backslash \omega_r^{\,2}{}_{\backslash}\right]$ are diagonal matrices containing the modal damping constants and modal natural frequencies squared, respectively. The mode matrix *[Φ]* is N_pxN and forces *{F}* are applied at any of the N_p physical coordinates.

Once the equations of motion for the subsystems are defined, they can be easily joined simply by defining constraints between the subsystems. For example, consider joining two subsystems A and B whose individual models are defined in the form of Eq. (1), having N_A and N_B modes and N_{pA} and N_{pB} physical coordinates respectively. We shall follow the notation in Ginsberg [3] for simplicity, although it is more efficient to implement this using Finite Element assembly methods. The total set of equations of motion are

$$\begin{bmatrix}[I_A] & 0\\ 0 & [I_B]\end{bmatrix}\begin{Bmatrix}\ddot{q}_A\\ \ddot{q}_B\end{Bmatrix}+\begin{bmatrix}\left[\backslash 2\zeta_r\omega_{r\backslash}\right]_A & 0\\ 0 & \left[\backslash 2\zeta_r\omega_{r\backslash}\right]_B\end{bmatrix}\begin{Bmatrix}\dot{q}_A\\ \dot{q}_B\end{Bmatrix}+\begin{bmatrix}\left[\backslash \omega_r^{\,2}{}_{\backslash}\right]_A & 0\\ 0 & \left[\backslash \omega_r^{\,2}{}_{\backslash}\right]_B\end{bmatrix}\begin{Bmatrix}q_A\\ q_B\end{Bmatrix}=$$

$$=\begin{bmatrix}[\Phi_A]^T & 0\\ 0 & [\Phi_B]^T\end{bmatrix}\begin{Bmatrix}F_A\\ F_B\end{Bmatrix}$$

$$\begin{Bmatrix}y_A\\ y_B\end{Bmatrix}=\begin{bmatrix}[\Phi_A] & 0\\ 0 & [\Phi_B]\end{bmatrix}\begin{Bmatrix}q_A\\ q_B\end{Bmatrix} \tag{2},$$

where *0* denotes a matrix of zeros of the appropriate dimensions.

These systems are to be joined in some way. The connections can usually be described by linear constraints between the physical degrees of freedom in the following form

$$\left[a_p\right]\begin{Bmatrix}y_A\\ y_B\end{Bmatrix}=\{0\} \tag{3}.$$

These in turn couple the modal degrees of freedom *{q}* as follows

$$\left[a_p\right]\begin{bmatrix}[\Phi_A] & 0\\ 0 & [\Phi_B]\end{bmatrix}\begin{Bmatrix}q_A\\ q_B\end{Bmatrix}=[a]\begin{Bmatrix}q_A\\ q_B\end{Bmatrix}=\{0\} \tag{4},$$

where *[a]* is an N_cx(N_A+N_B) matrix of constraints and N_c is the number of constraints.
Equations (2) and (4) define a correct set of equations of motion and could be used to simulate the response of the system to a variety of inputs. However, not all of the generalized coordinates in Eq. (2) are truly free, the system only has (N_A+N_B) - N_c degrees of freedom, so it is beneficial to condense the equations of motion to an unconstrained set. To do this, one must first define which modal coordinates $\{q_c\}$ will be constrained and which will remain unconstrained $\{q_u\}$. The procedure is simpler if these are placed at the top of the generalized coordinate vector.

$$\begin{Bmatrix}q_A\\ q_B\end{Bmatrix}=[P]\begin{Bmatrix}q_c\\ q_u\end{Bmatrix} \tag{5}$$

This choice, if done acceptably, does not affect the final results since only the physical degrees of freedom are meaningful in the combined system. Ginsberg suggests that this be done manually with a sorting matrix *[P]* that moves some of the modal coordinates, perhaps the last few modes for each subsystem, to the top of the generalized coordinate vector and assigns them as

constrained generalized coordinates. The previous equation is combined with Eq. (4) resulting in the following

$$[a][P]\begin{Bmatrix} q_c \\ q_u \end{Bmatrix} = [\hat{a}]\begin{Bmatrix} q_c \\ q_u \end{Bmatrix} = \begin{bmatrix} \hat{a}_c & \hat{a}_u \end{bmatrix}\begin{Bmatrix} q_c \\ q_u \end{Bmatrix} = \{0\} \qquad (6)$$

that is solved as follows to express the constrained generalized coordinates in terms of the unconstrained.

$$\{q_c\} = -[\hat{a}_c]^{-1}[\hat{a}_u]\{q_u\} \qquad (7)$$

Unfortunately, an incorrect choice in constrained generalized coordinates can result in a singular matrix $[\hat{a}_c]$ meaning that Eq. (6) cannot be solved for the particular choice of constrained generalized coordinates. This is best illustrated by an example:

Example: Choosing Constrained Generalized Coordinates

Consider joining two one dimensional systems at a single point. The constraint matrix $[a_p]$ *consists of a value of 1 and -1 at the two coordinates that are to be joined. The resulting* $[a]$ *matrix is then*

$$\left[\begin{bmatrix} \Phi_{y_c 1} & \cdots & \Phi_{y_c N_A} \end{bmatrix}_A \quad -\begin{bmatrix} \Phi_{y_c 1} & \cdots & \Phi_{y_c N_B} \end{bmatrix}_B\right]\begin{Bmatrix} q_A \\ q_B \end{Bmatrix} = [a]\begin{Bmatrix} q_A \\ q_B \end{Bmatrix} = \{0\} \qquad (8),$$

where y_c *indexes the row of the mode matrices corresponding to the physical coordinates that are being coupled. One generalized coordinate must now be defined as the constrained coordinate and the preceding equation will be solved for that coordinate in terms of the others as done in Eq. (7). Suppose that we assign the first modal coordinate of the A system* $(q_1)_A$ *as constrained. It is found in terms of the other generalized coordinates as*

$$(q_1)_A = -(\Phi_{y_c 1})^{-1}\left[\begin{bmatrix} \Phi_{y_c 2} & \cdots & \Phi_{y_c N_A} \end{bmatrix}_A \quad -\begin{bmatrix} \Phi_{y_c 1} & \cdots & \Phi_{y_c N_B} \end{bmatrix}_B\right]\begin{Bmatrix} (q_{2:N_A})_A \\ q_B \end{Bmatrix} \qquad (9).$$

It is now clear that this is not possible if the mode coefficient for this mode at the connection point $(\Phi_{y_c 1})$ *is zero. When structures are joined at multiple points the analogous situation occurs when the matrix* $[\hat{a}_c]$ *is singular.*

2.1.1. Maximum Rank Coordinate Choice

When the choice of constrained generalized coordinates results in a singular matrix $[\hat{a}_c]$, one recourse is to simply choose a different set of constrained generalized coordinates [3]. The authors instead devised the following scheme, which has been named the Maximum Rank Coordinate Choice (MRCC), that defines a set of constrained coordinates that ensure that $[\hat{a}_c]$ will be nonsingular unless such a choice is impossible. The authors are not aware of another method for assuring that the constrained generalized coordinates are well chosen. The MRCC method begins by finding the singular value decomposition (SVD) of the constraint matrix *[a]* as follows

$$[a] = [U_a][S_a][V_a]^T \qquad (10).$$

(According to the definition of the SVD, $[U_a]$ and $[V_a]$ are orthogonal matrices and $[S_a]$ is a diagonal matrix of singular values in order of decreasing magnitude.) Then let $[P]=[V_a]$ and by Eq. (6) and because $[V_a]$ is an orthogonal matrix,

$$\left[\hat{a}\right] = [U_a][S_a] \qquad (11).$$

The choice of *[P]* has resulted in the largest singular values of *[a]* and their associated singular vectors being placed in the leading columns of $\left[\hat{a}\right]$. As a result, each column of $\left[\hat{a}_c\right]$ is linearly independent, and in fact orthogonal to every other column, so it can always be inverted and the constrained generalized coordinates can always be found in terms of the unconstrained via Eq. (7), so long as the constraint matrix is of rank N_c.

One can now find a reduced set of equations of motion for the unconstrained generalized coordinates by noting that

$$\begin{Bmatrix} q_A \\ q_B \end{Bmatrix} = \left[P\right] \begin{bmatrix} -\left[\hat{a}_c\right]^{-1}\left[\hat{a}_u\right] \\ \left[I_{(N_A+N_B-N_c)}\right] \end{bmatrix} \{q_u\} = \left[B\right]\{q_u\} \qquad (12).$$

The reduced equations of motion then become

$$\begin{aligned} &\left[M\right]\{\ddot{q}_u\} + \left[C\right]\{\dot{q}_u\} + \left[K\right]\{q_u\} = \{Q\} \\ &\begin{Bmatrix} y_A \\ y_B \end{Bmatrix} = \begin{bmatrix} \left[\Phi_A\right] & 0 \\ 0 & \left[\Phi_B\right] \end{bmatrix} \left[B\right]\{q_u\} \end{aligned} \qquad (13),$$

where

$$\left[M\right] = \left[B\right]^T \begin{bmatrix} I_{N_A} & 0 \\ 0 & I_{N_B} \end{bmatrix} \left[B\right] \quad , \quad \left[C\right] = \left[B\right]^T \begin{bmatrix} \left[\backslash 2\zeta_r\omega_{r\backslash}\right]_A & 0 \\ 0 & \left[\backslash 2\zeta_r\omega_{r\backslash}\right]_B \end{bmatrix} \left[B\right]$$

$$\left[K\right] = \left[B\right]^T \begin{bmatrix} \left[\backslash \omega_r^{\,2}{}_{\backslash}\right]_A & 0 \\ 0 & \left[\backslash \omega_r^{\,2}{}_{\backslash}\right]_B \end{bmatrix} \left[B\right] \quad , \quad \{Q\} = \left[B\right]^T \begin{bmatrix} \left[\Phi_A\right]^T & 0 \\ 0 & \left[\Phi_B\right]^T \end{bmatrix} \begin{Bmatrix} F_A \\ F_B \end{Bmatrix}$$

(14).

One can now find the modes of the combined system by solving the eigenproblem $[K-\omega^2 M]\{\phi_r\}=0$. Note that all physical coordinates of the A and B systems have been retained, even though the presence of constraint equations implies that some of the physical coordinates might now be redundant. Typically one would remove any duplicate coordinates from $\{y_A\}$ and $\{y_B\}$ either before or after coupling the systems. All of the operations discussed in this section are easily automated. The authors can supply a Matlab function that implements this to interested researchers.

It is important to note that one could also use these procedures to remove a substructure. The only difference would be that the structure to be removed would have negative mass, stiffness and damping. In the context of finite element models this seems very reasonable since assembly of finite elements into a master system is clearly reversibly by simply changing the signs on the elements' contributions to the system matrices and repeating the assembly process. The more general case of coupling Ritz approximations to substructures that is considered here is similar in that one is removing mass, stiffness and damping from a system, yet the substructure models are global Ritz models rather than local finite elements.

2.2. Estimating Connection Point Responses

The problem investigated in the following sections involves coupling two beams together in bending and extension. The beams must be coupled in both displacement and rotation to yield a physically meaningful model, yet rotations are difficult to measure directly. This work addresses this issue by attaching a fixture to the end of the beam and measuring the translations at multiple points on the fixture. The effects of the fixture are removed using the substructuring procedure just outlined with negative signs on the subsystem matrices that are being removed. The measurement points on the fixture are shown with black arrows in Figure 1. These can be used

to estimate the connection point response using the modal filter described in the companion paper [12]. Unfortunately, this process was found to be very sensitive to measurement errors and/or errors in the fixture model, as described in Section 4.2.

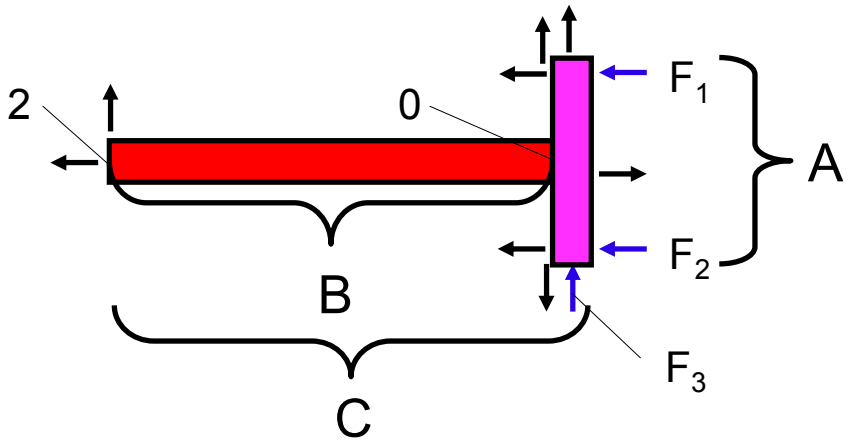

Figure 1: System under test consisting of Beam B and Fixture A. The measurement locations and directions on Fixture A are denoted with black arrows, the force application locations and directions with blue arrows.

One alternative is to constrain every measured point on the fixture of the C system to each corresponding point on the fixture model A, yet this assumes that all measurements are error-free, and was found to give erratic results. One would prefer a method that allows the fixture model to be joined to the measured substructure model in a least squares sense. The authors devised the following scheme to apply a least squares constraint to a pair of structures that does just this.

2.3. Modal Constraint for Fixture and Subsystem (MCFS)

One approach to joining subsystems A and C is to require equal displacement between all N_M of the measurement points as follows

$$\{x^C\}_M = \{x^A\}_M \qquad (15),$$

where the vectors denote the N_M x1 set of measurement points on C and A respectively. Some of the constraints above are redundant if the fixture model has fewer than N_M (active) degrees of freedom, yet eq. (15) implies that each equation is important. This can serve to amplify measurement errors since slight inconsistencies in the measurements enforce additional nonphysical constraints. One would prefer that eq. (15) instead be satisfied in a least squares sense so that errors could be averaged out. This can be done by instead satisfying the following weighted set of constraint equations,

$$W\{x^C\}_M = W\{x^A\}_M \qquad (16),$$

where the weighting matrix W has fewer rows than columns. To obtain meaningful results, the weighting matrix must be chosen to satisfy the essential constraints. If the fixture A is well described by a modal model with $N_A < N_M$ modes, then only N_A constraints are really needed to satisfy eq. (15) to within experimental precision. One can then make the following choice for W that couples the modal degrees of freedom of A to their approximation on C

$$pinv(\Phi^A)\{x^C\}_M = pinv(\Phi^A)\{x^A\}_M \qquad (17),$$

where $pinv(\Phi^A)$ denotes the pseudoinverse of the N_M x N_A mode matrix for system A. This represents a least squares solution to the constraint equation (15). This approach was found to give dramatically better results than attempting to use a modal filter to determine the connection point responses, as will be demonstrated in Section 4.2. This will be referred to as the Modal Constraint for Fixture and Subsystem (MCFS) method.

2.4. FRF Based Admittance Coupling

The Frequency Response Function (FRF) based coupling method is based on the same principles of balancing forces and ensuring compatibility at the interfaces of the substructures, but the operations are performed on FRFs rather than on models in the form of differential equations. The derivation for this system is presented in the companion paper [12] so only the final result will be repeated here:

$$\begin{aligned} HC_{00}^{-1} &= HB_{00}^{-1} + HA_{00}^{-1} \\ HB_{20} &= HC_{20} * HA_{00}^{-1} * (HA_{00} + HB_{00}) \\ HE_{21} &= HB_{20} * (HB_{00} + HD_{00})^{-1} * HD_{01} \end{aligned} \qquad (18).$$

The subscripts 0, 1 and 2 represent the connection point, force application point, and response point respectively. Hence, the FRF matrices HC_{00}, HB_{00}, HA_{00} are all three by three (x and y displacement and rotation about z). Equations (18) are applied at every frequency line of interest yielding the desired set of FRFs HE_{21}. The computation at each frequency line is independent and assumes nothing about the mathematical form of the systems except that they are linear. The admittance predictions here were obtained by reconstructing the FRFs for the C system from the measured modal parameters and condensing them to the connection point using the modal filtering procedure in [12].

3. System of Interest

The problem of interest, illustrated in Figure 2, consists of joining two beams B and D at the connection point labeled 0 to form the combined system E. System C represents physical hardware for which a test based model will be derived. Beam B is found by performing measurements on system C and then removing an analytical model of the fixture A attached to beam B from the measurements. The fixture serves a number of purposes. First, a small number of accelerometers are placed on the fixture and used to determine the rotation of the connection point 0. This is necessary since the beams must be coupled in both rotation and translation to yield a physically correct master structure. The fixture also serves to exercise the beam near the connection point so that the modes of the experimental system serve as a better basis to represent the behavior of the combined system. It is generally accepted that the free modes of a structure do not form an ideal basis for substructure coupling since free modes have zero moment and shear force at the interface. Furthermore, the additional mass on the end of the beam serves to bring more modes, and hence more information into the frequency band of interest. The admittance approach may also benefit if the mass of the fixture is on the same order as the effective mass of the final structure at the interface, since the net change produced by the admittance coupling would be smaller.

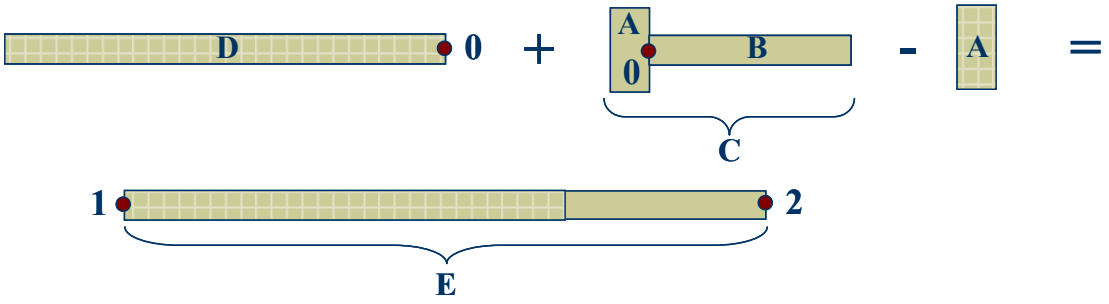

Figure 2: Schematic of substructure coupling problem. Experimental model for structure B is to be joined to an analytical (FE) model for structure D after the test fixture A attached to structure B is analytically removed.

Each beam is made of steel with nominal weight density 0.28 lb/in^3, modulus of elasticity 30e6 lb/in^2, height 0.75 in and width 1.0 in. The fixture is a 1.0 in by 1.0 in by 4.6 in long block of steel. The fixture was chosen to be long enough to minimize the errors in estimating the locations

of the excitation and measurement points. The fixture is bolted and adhered to beam B using a US ¼-28, grade 5 bolt and dental cement [12].

4. Results

4.1. Simulation Example

The CMS method was first applied to join simulated experimental and analytical models for two beams having the same properties as the experimental ones. This allows one to evaluate the performance of the CMS method in the absence of experimental error. Structures C and D were simulated using a finite element (FE) model with 40 beam elements per foot and the nominal dimensions of the beams. The fixture attached to beam B was modeled as a lumped mass, its mass and inertial properties computed from its density and dimensions and approximating the block as a solid rectangular bar. This neglects the accelerometers, their mounting blocks and the excitation pads shown in the figures in [12].

Two cases will be considered here. The first follows the schematic in Figure 2 where measurements are simulated on the mass loaded system C, the fixture A is analytically removed, and the resulting model for beam B is coupled to the FE model for D. This will be denoted the mass loaded (ML) case. The second case simulates measurements taken on the free-free structure B, when no fixture is attached at y_c, and then couples the result to the finite element model for D. This case will be denoted the free-free (FF) case.

Only axial motion of the beams will be considered for brevity. Similar results were obtained when the component models were joined in the lateral direction. Measurements are simulated in both cases by assuming that the modes of the experimental structure (C for ML case and B for FF case) are only known up to 10 kHz. In each case the modal natural frequency and the necessary mode shapes are assumed to have been measured perfectly. The data in the frequency band of interest consists of one rigid body mode and one elastic mode on the simulated experimental substructure (B or C) for both the FF and ML cases. Table 1 displays the natural frequencies of system C that are below 10kHz with 1.) the lumped-mass fixture (C-ML), 2.) the natural frequencies of C-ML after analytically removing the fixture (B-MR), which is an estimate for the free-free B system, and 3.) the natural frequencies of the system without the fixture (B-FF). The analytical procedure used to remove the lumped mass is not entirely accurate, as evidenced by the fact that the second B-MR natural frequency is not identical to the second B-FF natural frequency. This is to be expected, since the model for C from which the mass was removed consisted of only the rigid body mode and one elastic mode. The error decreases as more modes are included for beam C, with zero error being obtained when all 41 of beam C's axial modes are used to compute the free-free mode, in which case the modal model for the B-MR structure is complete and identical to the finite element model for the free-free beam.

Natural Frequencies (Hz)

Mode	C-ML (mass-loaded)	B-MR (mass removed)	B-FF (free-free)
1	0.0	0.0	0.0
2	5128.7	9425.2	8472.5

Table 1: Natural frequencies of mass-loaded system C (C-ML), free-free system B (B-FF) and natural frequencies of mass-loaded system C after analytically removing the fixture (B-MR).

Both the B-FF and the B-MR structures were then coupled to the FE model for the D structure resulting in the E system natural frequencies shown in Table 2. The result of coupling the complete finite element model for system B is also shown (FEA), which is taken to be the truth model, and the errors of the FF and ML cases are shown relative to the FEA case. The ML case shows very small errors for modes 2 and 3, yet larger errors for modes 4 and 5 than the FF case. Either method estimates all of the natural frequencies in the 10kHz frequency band with less than 4% error. It is interesting that the ML modes predict the natural frequencies of the

combined structure well, even though they did not accurately predict the first elastic natural frequency of the B system (after the end mass was removed.)

Natural Frequencies (Hz)

Mode	E-FEA	E-FF (free-free)	E-ML (mass-loaded)	Error (E-FF) (free-free)	Error (E-ML) (mass-loaded)
1	0.0	0.0	0.0	0.0%	0.0%
2	2824.8	2919.4	2829.7	3.3%	0.2%
3	5649.1	5860.6	5651.3	3.7%	0.0%
4	8472.5	8472.5	8678.5	0.0%	2.4%
5	11294.3	11758.9	12171.5	4.1%	7.8%

Table 2: Natural frequencies of combined system, E, using the full FEA model for system C (FEA), using free-free modes for C (FF) and using mass-loaded modes for system C (ML). The errors for the FF and ML cases are also shown relative to the full FEA model.

Figure 3 shows the first three mode shapes obtained for the combined system E using the full FEA model, and using the free-free modes and mass-loaded modes for system B. The mode shapes obtained using the ML modes for system B overlay the true FE modes almost exactly. On the other hand, when the FF modes are used, the mode shapes show noticeable errors, especially near the connection point. The errors in the mode shapes for the FF case are about 20% at most, whereas the natural frequency errors for the FF case showed only 4% maximum error. The FF mode shapes have zero slope at the connection point (24 inches), which is as one would expect since the shapes for the combined system are linear combinations of the FF mode shapes, and each FF mode shapes has zero axial force at its free end. The ML mode shapes do not suffer from this limitation since the mass on the connection point of the C system results in its mode shapes, and hence the B-MR mode shapes, having nonzero slope at the free end.

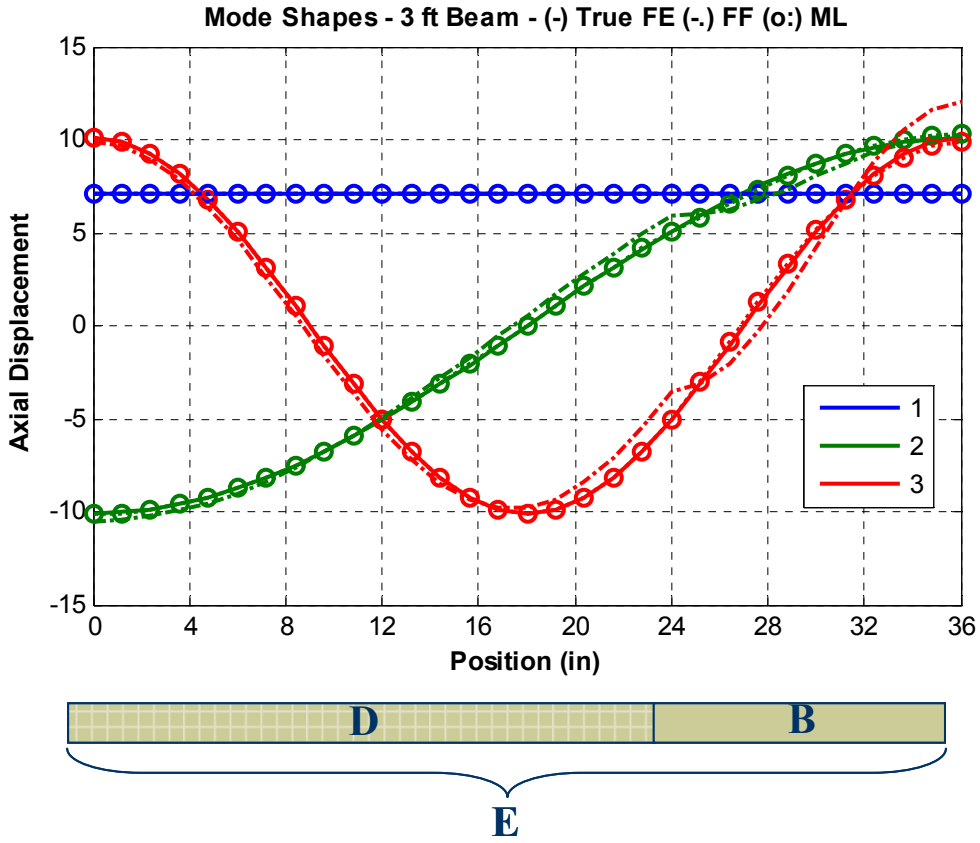

Figure 3: First three mode shapes for combined system E using full FEA model for beam B (solid lines), using free-free modes for beam B (dash-dot lines) and using mass loaded modes for beam B (dotted lines and circles).

4.1.1. Discussion

The analysis just described assumed that all of the modes of both structures were available below 10 kHz. In the problem of interest the measurable frequency range is actually 0 to 6400 Hz, as discussed in [12]. If this were used in the previous analysis, the FF model for beam B would not have any elastic modes in the frequency band of interest while the ML model would still have one mode in the frequency band. This was found to increase the error in the FF natural frequencies for the E system to 9.3% and 21.4% for the first two elastic modes. The 10 kHz band was used in the preceding in order to obtain a more uniform comparison between the performance of mass-loaded and free-free modes. However, in practice, one advantage of mass loaded interfaces is that they can reduce the frequencies of a system's modes, bringing more modes into the measurable frequency range.

4.2. Experimental Application

The modal substructuring method was also applied to an experimental system. The details of the experiment and data acquisition are provided in [12]. The basic problem is identical to that presented in the previous section; an experimental model of beam B is to be coupled to an analytical model for beam D. The combined equations of motion are

$$\begin{bmatrix} -[I_A] & 0 & 0 \\ 0 & [I_C] & 0 \\ 0 & 0 & [I_D] \end{bmatrix} \begin{Bmatrix} \ddot{q}_A \\ \ddot{q}_C \\ \ddot{q}_D \end{Bmatrix} + \begin{bmatrix} -\left[\backslash 2\zeta_r \omega_{r\backslash} \right]_A & 0 & 0 \\ 0 & \left[\backslash 2\zeta_r \omega_{r\backslash} \right]_C & 0 \\ 0 & 0 & \left[\backslash 2\zeta_r \omega_{r\backslash} \right]_D \end{bmatrix} \begin{Bmatrix} \dot{q}_A \\ \dot{q}_C \\ \dot{q}_D \end{Bmatrix} + \cdots$$

$$\begin{bmatrix} -\left[\backslash \omega_r^{\,2} \backslash \right]_A & 0 & 0 \\ 0 & \left[\backslash \omega_r^{\,2} \backslash \right]_C & 0 \\ 0 & 0 & \left[\backslash \omega_r^{\,2} \backslash \right]_D \end{bmatrix} \begin{Bmatrix} q_A \\ q_C \\ q_D \end{Bmatrix} = \begin{bmatrix} [\Phi_A]^T & 0 & 0 \\ 0 & [\Phi_C]^T & 0 \\ 0 & 0 & [\Phi_D]^T \end{bmatrix} \begin{Bmatrix} F_A \\ F_C \\ F_D \end{Bmatrix}$$

(19).

These are supplemented with six constraint equations enforcing equal axial, lateral and rotational displacement at the connection point. The constraint equations are used to reduce the equations of motion to an unconstrained set using the MRCC method.

The analytical model for beam D is an Euler-Bernoulli solution for a beam in bending and (a rod in) extension. The Euler-Bernoulli beam equation was solved for the first 10 elastic modes and these were supplemented with the first 9 axial modes found by solving the rod equation. These 19 modes were augmented with the three rigid body modes resulting in a 22 mode model for beam D. The natural frequencies of this model were adjusted to match those found by testing a 24-in beam in the laboratory.

System C consists of beam B with the fixture A attached. A modal test was performed on system C with free-free boundary conditions and all of the bending and axial modes below 6400 Hz were extracted. An additional axial mode at 8293 Hz was also extracted. Measurements on the fixture A attached to beam B were used to deduce the displacement and rotation of the connection point (y_c in Figure 2) as discussed in [12]. Models for beam B were obtained by subtracting a model for the fixture A from the modal model for system C. Both rigid and elastic models for the fixture were considered, as described in the following two subsections.

4.2.1. Rigid Fixture

The first model for the fixture treated it as a rigid body with a mass of 3.33e-3 lb-s^2/in and moment of inertia 6.99e-3 lb-in-s^2 about the axis perpendicular to the plane containing the beam and the fixture. The mass normalized rigid body mode shapes for the fixture were computed at the measurement points using the known mass. This information was used to generate a 3-mode model for the fixture as in Eq. (1) with $\omega_n = 0$. The mass matrix for this system was a negative identity matrix, since the intent is to subtract the fixture A from the C system. The negative fixture model was coupled to the Beam C model and the Beam D model according to Eq. (2) with six constraint equations to enforce equal axial, lateral and rotational displacement at the connection point.

The resulting model for the combined system E was then used to compute the FRFs (HE_{21}) between response at point 2 due to force at point 1 (see Figure 2) in both the axial and lateral directions. Figure 4 shows the lateral force to lateral response HE_{21} FRF. The result of using the Admittance procedure from [12] is also shown, as well as the analytical prediction computed by solving the Euler-Bernoulli beam equation for a 36 in beam. Both predictions agree with the analytical result almost perfectly, although there are some very small frequency differences between the predictions and the analytical result. The modal substructuring (MS) result also shows a few small amplitude spikes at 2400 and 5200 Hz, which correspond to the frequencies of the axial modes of the beam.

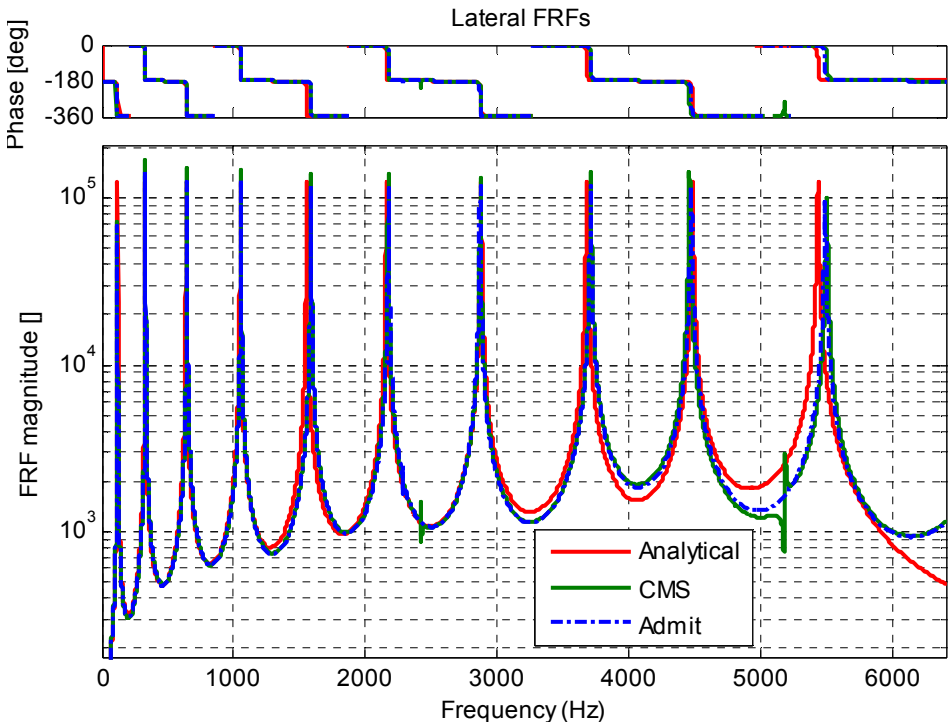

Figure 4: Lateral FRF predicted by modal substructuring (MS) and admittance using a rigid fixture model and that predicted analytically.

The axial force to axial response HE_{21} FRFs predicted by CMS and admittance are shown in Figure 5 and compared with the analytical prediction. The CMS and Admittance predictions are very similar, yet both underestimate the natural frequencies of both axial modes. There were some differences in the way these methods were implemented [12], otherwise one would expect identical results so long as numerical ill-conditioning is not encountered.

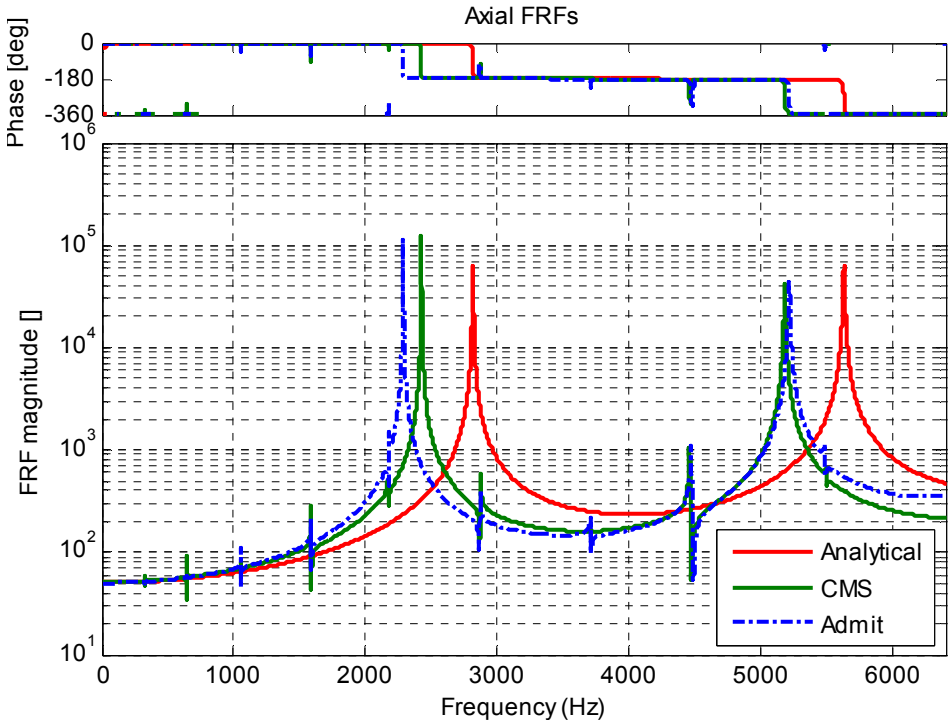

Figure 5: Axial FRF predicted by modal substructuring and admittance using a rigid fixture model and that predicted analytically.

It was noted that the modal substructuring approach returned purely imaginary natural frequencies for two of the modes of the E system. The absolute value of the first was very small suggesting that it should have been a rigid body mode. This eigenvalue was assigned a natural frequency of zero and retained. The other had a very large natural frequency, well beyond the frequency band of interest, so it was discarded along with its mode vector. Further investigation found that one of the eigenvalues of the E system mass matrix was -0.0115 (in modal coordinates). Most of the eigenvalues of the mass matrix were unity, so this value was relatively small. This is clearly non-physical since it would imply that the system could have negative kinetic energy for a certain combination of the modal amplitudes. Other than these two features, the model obtained by MS was physical.

It is much more difficult to evaluate the physicality of the admittance prediction. There are properties that one could test, such as whether the imaginary part of the FRF matrices are always positive at the driving point [13], yet this must be done at every frequency line.

4.2.2. Elastic Fixture Joined at Connection Point

A 3D finite element analysis of the beam-fixture subsystem C revealed that the fixture was significantly flexible in the system's axial direction. This can be accounted for by treating the fixture as elastic and subtracting an elastic fixture model from the measured model for C. A simple elastic model for the fixture was created by modeling the fixture with a single bending mode. In doing so, it was thought that since beam B is coupled to the fixture over a 0.75-in by 1-in area, the connection might restrain bending in fixture over that area. Hence, the connection was approximated by modeling the fixture as a guided free beam with length (4.6-0.75)/2-in with a mass at the guided end equal to the mass of the 0.75/2 in^3 segment of the fixture that was fixed to the end of the beam. Analytical solution of the Euler-Bernoulli beam equation for this guided-free model resulted in a first natural frequency of 17.3 kHz. This model is not expected to be highly accurate since the beam is not long and slender as required by the Euler-Bernoulli theory, although it might be sufficiently accurate to account for the flexibility of the fixture adequately.

Figure 6 shows the lateral FRFs predicted for the combined system using the flexible beam model in both the admittance and modal substructuring approaches, compared with the

analytical result. Both results agree very well with the analytical model, as they did in Figure 4 for the rigid fixture.

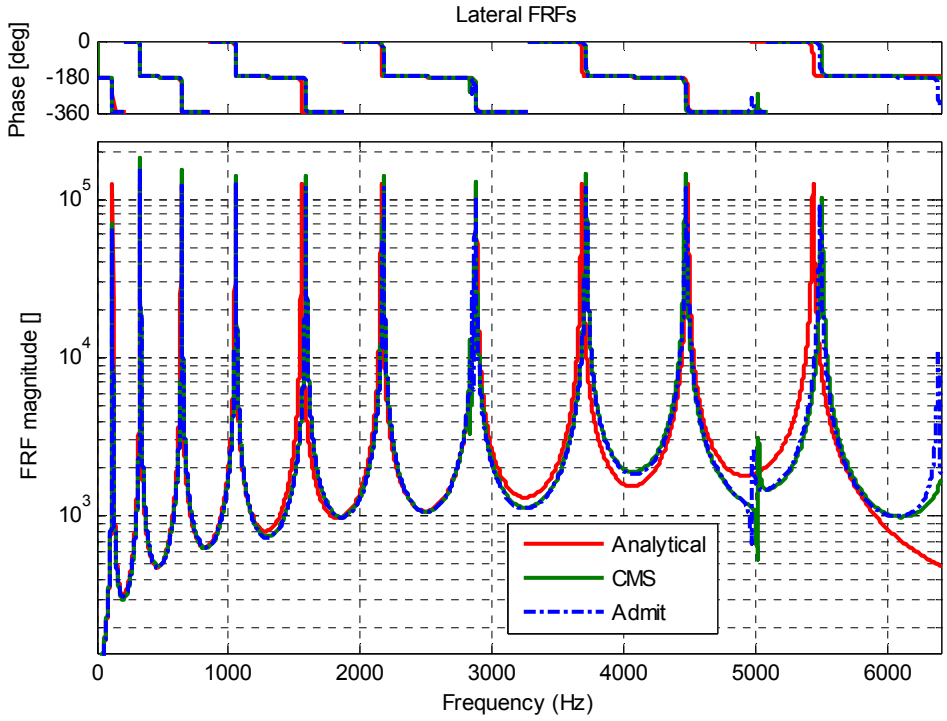

Figure 6: Lateral FRF predicted by modal substructuring and admittance using an elastic fixture model and that predicted analytically.

The elastic fixture model has a much more significant effect on the axial modes, as illustrated in Figure 7, which compares the predicted FRFs using the one-elastic mode fixture with the analytical prediction. Comparison to rigid fixture result in Figure 5 reveals that the natural frequency of the first axial mode is predicted much more accurately with this elastic fixture model for both the modal substructuring and admittance approaches. On the other hand, the second axial mode is even more severely underestimated when the elastic fixture model is used. Both the MS and Admittance models predict an anti-resonance near 5500 Hz. This is clearly non-physical since Beam E is a free-free structure. An anti-resonance would imply that forces internal to the beam can cause zero displacement at the response point (a vibration absorber), and this is not possible at a free end since the vibration absorber would have to be located beyond the end of the beam.

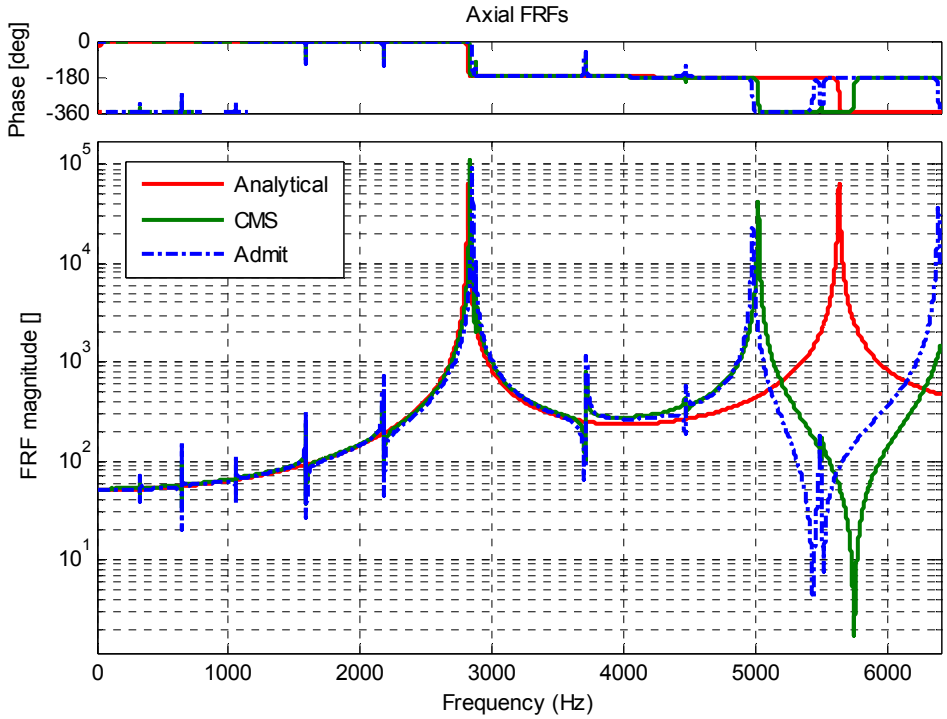

Figure 7: Axial FRF predicted by modal substructuring and admittance using an elastic fixture model and that predicted analytically.

The modal substructuring method returned three complex natural frequencies when the flexible fixture was used. The first had a small absolute value, so it was assumed to be a rigid body mode and it was assigned a natural frequency of zero. The next two were a complex conjugate pair at $8951.1+2450.6i$ Hz. Their accompanying mode vectors were also a complex conjugate pair whose coefficients were about four times stronger in the axial direction than they were in the lateral. It was also noted that the mass matrix for the E system had all positive eigenvalues except one that was equal to -1. The corresponding eigenvector for that eigenvalue was a vector of zeros in physical coordinates. The eigenvalue of -1 is clearly nonphysical, as it would imply that a state exists that possesses negative kinetic energy. On the other hand, it is interesting that the accompanying pattern of motion exists only internally as it corresponds to zero motion at all of the system's measurement points.

The fixture mode shapes were used in two ways in these analyses. First, they were used to solve a least squares problem to determine the connection point rotation and translation from the responses measured by the five accelerometers on the fixture. This is discussed in more detail in the companion paper [12]. Second, they were part of the dynamic model for the fixture that was subtracted from the C system to estimate the B system. The analysis in this section was repeated using the flexible mode shape of the fixture in the modal filtering step, but omitting it from the modal model for the fixture that was subtracted from system C. The results obtained were virtually identical to those presented in Figures 6 and 7. The differences between Figures 4 and 6 and Figures 5 and 7 must then be due to differences in the estimates of the connection point translation and rotation mode shapes rather than to differences in the subcomponent models. Interestingly, this alternative analysis (when the elastic mode of the fixture was omitted from the CMS model) yielded a positive definite mass matrix and only two complex natural frequencies, both of which had very small magnitudes and hence were assumed to be rigid body modes.

4.2.2.1. Discussion

The results presented in the previous sections show that the modal substructuring approach gives excellent results in the lateral direction; the lateral FRFs of the E system agree

very well, implying that the E system's bending modes are predicted very accurately. The results are also quite good in the axial direction, except for the last axial mode that is predicted to be at a 10% lower frequency than it actually is. The magnitudes of the errors in this mode in both Figures 5 and 7 are much larger than one would expect based on the results of the simulation presented in Section 4.1. It was noted that one could obtain results that were virtually identical to those in Figures 6 and 7 by using the flexible mode of the fixture model in the modal filtering step and omitting it from the system model. The additional flexible mode had a significant effect on the modal filter that was used to estimate the connection point responses. The estimate of the first axial frequency improved when this mode was added to the modal filter, although perhaps at the expense of the second. These observations seem to suggest that the errors encountered in estimating the natural frequencies of the axial modes were not due to deficiency in the size of the modal models for the A and C systems but in the difficulty associated with accurately measuring the mode shapes at the connection point.

4.2.3. Elastic Fixture Joined Using MCFS Method

The MCFS method in equation (17) was also employed to couple the negative fixture model A to the C component at all of the measurement points (in a least-squares sense). The D component was coupled to the connection point degrees of freedom of the A component of the combined A-C system. The resulting predicted axial FRFs are shown in Figure 8. The bending FRFs were similar to those presented previously in Figures 4 and 6. The least squares method predicts the axial FRF very accurately, with excellent agreement at both axial natural frequencies. This analysis yielded a combined system mass matrix having one negative eigenvalue and the overall system had one complex rigid body mode and a pair of complex natural frequencies at 13 kHz. It was also noted that nearly identical results were obtained when the fixture model was replaced with 1.) an Euler-Bernoulli free-free beam model (4.6-in long), 2.) a 2.3-in long guided-free Euler-Beronoulli beam model, and 3.) the 1.925-in guided-free model described previously that was used in Figures 4 through 8. The Admittance result and the CMS result found using a modal filter to determine connection point responses (Figure 7) both changed significantly in the vicinity of the second axial mode depending on which fixture model was used.

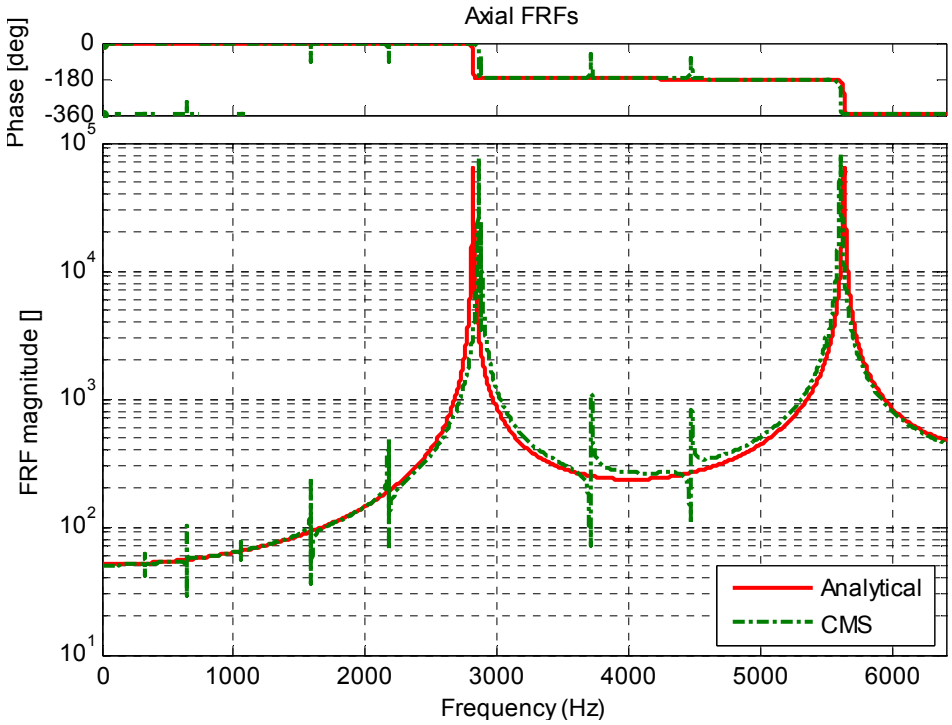

Figure 8: Axial FRF predicted by CMS using an elastic fixture model and coupling A and C using the least squares method. The analytical FRF is also shown.

4.2.3.1. Discussion

Sections 4.2.2 and 4.2.3 presented the results of coupling the analytical elastic fixture model to the measured C system in two different ways. The first used a modal filter to estimate the three connection point coordinates from the measurements on the C system. The second also used a modal filter based on the fixture model, but coupled the four modal coordinates of the A system to their representation on the C system. The A system is described by a four mode model, so the amplitude of each modal contribution can be determined in a least squares sense from the six measurement points using the known mode matrix (i.e. $\{q^A\} = pinv(\Phi^A)\{x^A\}_M$ since Φ^A is N_mxN_A and $N_m > N_A$.) However, the modal amplitudes cannot be determined uniquely from the instantaneous connection point displacements alone because there are only three connection point DOF and four modes. If the model for the fixture (A) were known perfectly, then knowledge of the motion at the connection point and the fixture model would be sufficient to determine the motion of the rest of the fixture as a function of time. This is related to the frequency domain inverse method for determining the forces acting on a structure and its variants [14, 15], which are known to be quite sensitive to errors in the system model. It seems logical that it might be easier to constrain the motion of C to match that of A using four points on the perimeter of the fixture rather than using only the three degrees of freedom at the connection point even though both are theoretically possible. Hence, it is not really surprising that the MCFS method that employs one constraint per mode to directly constrain the modes of the A system to their projection onto C is more accurate and much more robust than constraining the structures at the connection point alone when the fixture (A) has more than three active modes.

This is not so much an issue when one is interested only in combining substructures since a physically meaningful result is obtained so long as the boundaries of each substructure are properly joined. On the other hand, when one wishes to subtract a component from a measured model, one must assure that all of the modes the component model are adequately constrained to the corresponding system measurements or the result may be highly sensitive to the component model.

4.2.4. Remarks

Before concluding, it should be noted that a close inspection of the C system's mode shapes revealed that the motion of the fixture in the second axial mode included some rotation about the connection point. This suggests either that the fixture was not attached exactly in line with its center of mass or that the mass of the accelerometers, their mounting blocks and the force pads (which was neglected in the fixture model) was sufficient to cause asymmetry. This may have contributed to some of the difficulties described in the preceding sections.

It was also noted that complex natural frequencies were encountered and that the combined system mass matrix was not always positive definite. This is somewhat troubling since it leads to a non-physical model, yet it should be expected when one subcomponent is removed from a system because there is always the possibility that the removed mass or stiffness could be greater than what was originally in the system. This is the analog to high frequency errors in natural frequency predictions when two finite-length modal models are joined. One would hope that these errors would only affect modes that are out of the frequency band of interest, as is always the case when joining structures. This seemed to be the case here since most of the complex natural frequencies were above the frequency band of interest. The other complex natural frequency had small magnitude, appearing to be the missing rigid body mode, so it seemed quite reasonable to set it to zero. Future efforts will be directed at modeling the fixture more accurately to avoid or minimize these types of errors.

5. Conclusions

The CMS method has been compared to the impedance or admittance coupling method for a simple structure comprised of two beams joined at their ends. The general theory employed was described as well as a novel method that can be used to avoid ill conditioning when eliminating constrained degrees of freedom from the combined system model, dubbed the Maximum Rank Coordinate Choice (MRCC). The modal substructuring method was then demonstrated on two systems modeled using finite elements, demonstrating the utility and high accuracy of the methods, especially when mass-loaded-interface modes are employed. The companion paper [12] showed that poor results were obtained when admittance coupling was performed on the measured FRFs. On the other hand, good results were obtained using both the CMS and admittance approaches when the admittance approach employed reconstructed Frequency Response Functions (FRFs). A familiar rule of thumb that states that one should use all of the subcomponents' modes covering a frequency band of 1.5 to 2.0 times the frequency band of interest for the assembly. Taken in reverse, this suggests that since the subcomponents in this study were only described from 0 to 6400 Hz by the modal models used, the results should only be trusted out to 3200 or 4200 Hz. Significantly better results were obtained in the axial direction when the Modal Constraint for Fixture and Substructure (MCFS) method was employed, which coupled the modal coordinates of the fixture to their projection onto the C system. The MCFS method obtained excellent agreement over the entire 6400 Hz measurement band. The good performance of the MCFS method was attributed to the fact that direct constraint between all of the fixture modes and the measured component assures that the fixture model and the component are adequately constrained, even if the fixture model is less than perfect.

Some non-physicality was identified in the final combined system model found by the CMS method and its character and sources were investigated. It was noted that the methods available to evaluate the physicality of the admittance coupling results are somewhat more cumbersome because they must be applied at every frequency line. The modal substructuring method has the advantages of easy integration into existing finite element codes, a compact and easy to manipulate database for the experimental structure, and the fact that one can apply insight gained from the voluminous works on CMS, modal substructuring and the Ritz method.

6. References

[1] R. R. J. Craig, *Structural Dynamics*. New York: John Wiley and Sons, 1981.

[2] R. R. J. Craig and M. C. C. Bampton, "Coupling of Substructures Using Component Mode Synthesis," *AIAA Journal*, vol. 6, pp. 1313-1319, 1968.

[3] J. H. Ginsberg, *Mechanical and Structural Vibrations*, First ed. New York: John Wiley and Sons, 2001.
[4] D. J. Ewins, *Modal Testing: Theory, Practice and Application*. Baldock, England: Research Studies Press, 2000.
[5] D. J. Segalman, "Model Reduction of Systems with Localized Nonlinearities," Sandia National Laboratories, Albuquerque, NM SAND2006-1789, 2006.
[6] D. T. Griffith and D. J. Segalman, "Finite Element Calculations Illustrating a Method of Model Reduction for the Dynamics of Structures with Localized Nonlinearities," Sandia National Laboratories, Albuquerque, NM SAND2006-5843, 2006.
[7] D. R. Martinez, A. K. Miller, and T. G. Carne, "Combined Experimental and Analytical Modeling of Shell/Payload Structures," presented at The Joint ASCE/ASME Mechanics Conference, Albuquerque, NM, 1985.
[8] A. P. V. Urgueira, "Dynamic Analysis of Coupled Structures Using Experimental Data," in *Imperial College of Science, Technology and Medicine*. London: University of London, 1989.
[9] P. Ind, "The Non-Intrusive Modal Testing of Delicate and Critical Structures," in *Imperial College of Science, Technology & Medicine*. London: University of London, 2004.
[10] M. Imregun, D. A. Robb, and D. J. Ewins, "Structural Modification and Coupling Dynamic Analysis Using Measured FRF Data," presented at 5th International Modal Analysis Conference (IMAC V), London, England, 1987.
[11] L. A. Simmons, G. E. Smith, R. L. Mayes, and D. S. Epp, "Quantifying Uncertainty in an Admittance Model Due to a Test Fixture," presented at 23rd International Modal Analysis Conference (IMAC XXIII), Orlando, Florida, 2005.
[12] R. L. Mayes and E. C. Stasiunas, "Lightly Damped Experimental Substructures for Combining with Analytical Substructures," presented at 25th International Modal Analysis Conference (IMAC XXV), Orlando, Florida, 2007.
[13] T. G. Carne and C. R. Dohrmann, "Improving Experimental Frequency Response Function Matrices for Admittance Modeling," presented at 24th International Modal Analysis Conference (IMAC XXIV), St. Louis, Missouri, 2006.
[14] J. A. Fabunmi, "Effects of Structural Modes on Vibratory Force Determination by the Pseudoinverse Technique," *AIAA Journal*, vol. 24, pp. 504-509, 1986.
[15] D. C. Kammer and A. D. Steltzner, "Structural identification using inverse system dynamics," *Journal of Guidance Control and Dynamics*, vol. 23, pp. 819-825, 2000.